

Retrieval of IVUS Images Using Contextual Information and Elastic Matching

Jaume Amores,* Petia Radeva†

*Centre de Visió per Computador (CVC), Department Informàtica,
Universitat Autònoma de Barcelona, Bellaterra 08193, Spain*

We present a content-based image retrieval system of medical images of bodies with high elasticity, that is, high inter- and intrasubject variability in shape. The system is based on a rich feature space that is able to describe all the relevant aspects of an image, including local, global, and contextual information. For including relative spatial relations between the structures (i.e., contextual information) we do not need to obtain very accurate segmentations of the image, in contrast to the majority of methods employed for this kind of description. We also obtain invariance to spatial deformations of the same type of object along different instances. This is achieved by applying efficient registrations of the images before their comparison. The incorporation of all these components represents an innovative and powerful way of comparing and retrieving medical images. Validated results are reported on a database of 168 intravascular ultrasound images, showing the appropriateness of our approach for images of such high complexity. © 2005 Wiley Periodicals, Inc.

1. INTRODUCTION

The increasing volume of image data as a means of representing information in several applications makes it necessary to use efficient and meaningful retrieval systems of images. The poor performance of textual entries for representing this information leads to the necessity of using content-based image retrieval (CBIR) systems. Typical examples of applications with a high volume of images are remote sensing and medical image applications.

In content-based image retrieval systems, the images are first described in some feature space that attempts to take all the relevant information of each image, and then compares the images in this feature space based on an appropriate similarity measure. Thus, one of the most important aspects is how we design such a feature space for describing the relevant information in a compact manner. The

*Author to whom all correspondence should be addressed: e-mail: jaume@cvc.uab.es.

†e-mail: petia@cvc.uab.es.

majority of current CBIR systems^{1,2} use only global descriptors, such as histograms of color or texture, as a way of summarizing the overall content of the image. For differentiating among images in which discriminant information is localized in small regions, some authors begin to include local information in their feature space.^{3,4} Relative spatial information is also important for describing an image in terms of its objects and their spatial relations. For example, if we are looking for faces, we can describe them as containing two eyes beside each other, one nose below and in the middle, and one mouth below the nose. In medical image domains the relative spatial distribution of the pathological structures play important roles in diagnosis. For including this information Petrakis and Faloutsos⁵ use attributed relational graphs representing the structures by nodes with their attributes, and their spatial relations by links with their attributes. They apply this to retrieve magnetic resonance images (MRI). Chang et al.⁶ use two-dimensional (2-D) strings for representing this contextual information in a general retrieval framework. These descriptors require almost exact segmentations, so that the structures must be segmented manually, in general. Another way of including contextual information is the use of spatial histograms or correlograms.⁷⁻⁹ These correlograms have been applied to describe the distribution of color along with its spatial relations⁷ or the relative distribution of the points in a curve in shape matching and retrieval.⁸

The same type of object can undergo spatial transformations along its different instances. For example, in 2-D images of 3-D objects, the shape and appearance of the object differ depending on the camera viewpoint. In this case it is appropriate to have a projective invariant comparison between images. In medical images such as intravascular ultrasound (IVUS), there is a high intra- and inter-subject variability in the same type of structure, making it necessary to take into account invariance to elastic transformations. Few works try to take into account this transformation invariance. Dahmen et al.¹⁰ uses a comparison between images that is invariant to local deformations and small global transformations. Their model allows an object to be deformed to a completely different object, not taking into account any smoothness restriction in the mapping. Robinson et al.¹¹ make a registration of two contours, making the comparison invariant to elastic transformations. Their registration algorithm is particular for mappings between closed contours and does not take into account smoothness restrictions either. Liu et al.¹² makes registration of brain volumes before their comparison. They use particular properties of the brain such as its symmetry for performing this registration. The registration uses an affine transformation; therefore it does not accommodate for local (elastic) deformations.

We propose a retrieval system that incorporates all the relevant sources of information for describing the content of an image: local, global, and contextual information. All these types of information are included in a generalization of the correlograms or geometric histograms used in Refs. 7-9, among others. These descriptors allow us to describe statistics over the features (such as color) in the image, taking into account their spatial relationship. The features in our case consist of the different types of structures existing in the image, using local information for this purpose. The relative distribution of these structures is integrated into the generalized correlogram without needing to perform exact segmentations of the

structures. This is very important, because it is accepted nowadays that there are no algorithms able to make exact segmentations of images in a general domain. Our correlograms incorporate all types of information mentioned before. Local information is extracted from features associated to each local structure and provide information about its type of structure. Contextual information is incorporated by taking into account the relative spatial distribution of these local features. Finally global information is obtained as a result of considering the local features over wide neighborhoods embracing the whole image. Finally, we provide two different definitions of the correlogram: a 2-D correlogram that uses the same spatial quantization as the one of Belongie et al.,⁸ and a unidimensional shape-invariant correlogram.

Along with this rich feature space we provide invariance to elastic transformations by performing elastic matching of the images before their comparison. We use thin-plate splines based on small sets of landmarks. This makes our algorithm efficient, as opposed to registration methods such as the one by Bajcsy and Kovacic¹³ that use expensive PDE approaches based on all the pixels of the image. Thin-plate splines not only model global and local (elastic) deformations, but also incorporate a smoothness component in the transformation that avoids changes in topology of the object (i.e., misregistration). The registration step also provides measures of similarity between the images, such as the degree of alignment achieved and the amount of deformation necessary to align them. These measures are later incorporated into the final comparison of the images along with the similarity between their correlograms.

We apply this retrieval algorithm to a database of IVUS images. IVUS is a powerful imaging modality for analysis and diagnosis of coronary vessels. In this modality, we obtain a cross-sectional view of the artery by inserting a catheter into it (see Ref. 14 for a wide introduction). The structure and composition of atherosclerotic plaques play important roles in coronary artery disease study and in the outcomes of coronary interventions; hence, a system that accurately retrieves these cases is interesting. In Figure 1 we can see an IVUS image with the catheter in its center represented by a circle with high intensity and a point (the tip) in its center. Around the catheter there is the blood in the lumen of the vessel. In this picture there are two kinds of biological structures: the adventitia tissue, represented by a big region of high intensity and fine texture, and two calcium plaques, represented by thin regions of intensity equal to or greater than the adventitia and with dark regions beyond it.

The article is organized as follows: Section 2 describes the feature space, Section 3 the registration method, Section 4 the comparison between images after their registration, and Section 5 shows the results obtained. The article finishes with conclusions and future work.

2. FEATURE SPACE

As mentioned before, our feature space must include all types of information relevant to describe the image. Thus, we include local, global, and contextual information, and we do so by using generalized correlograms. In the following we

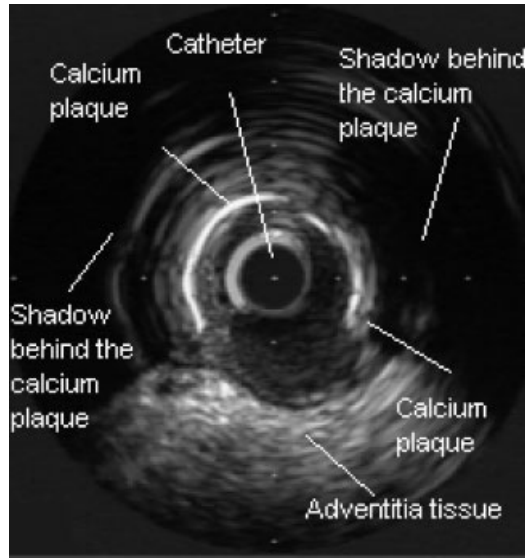


Figure 1. IVUS image with different structures.

explain how local information is represented, and then how we include it in generalized correlograms that also take into account global and contextual information. Our feature space is based on landmarks automatically extracted around discriminant regions of the image. For each landmark we associate descriptors that account for the type of structure in which it lies (local information), and the spatial organization of the structures around (contextual and global information). As we will explain later, we use this feature space not only for representing the content of the image in the retrieval similarity, but also for registering the images before their comparison. Using our generalized correlograms in the registration will allow us to make matchings taking into account local attributes of the structures as well as global properties (e.g., the size) and their context.

Coronary vessels present all their structures of interest around the interface between lumen and adventitia, what we call the wall of the vessel. Thus, in our case the set of characteristic points to be extracted from each image will be placed along this boundary. We first extract the catheter of the image, apply an anisotropic diffusion¹⁵ of the resulting IVUS image, and let a snake grow from its interior to the wall of the vessel. Finally, we sample the boundary points, and this will be our set of characteristic points. The next step will be to extract the feature vectors associated to each characteristic point. We compute local feature vectors associated to each characteristic point and then, based on them, we perform classification by Nonparametric Discriminant Analysis¹⁶ and K-Nearest Neighbors. This classification assigns a label to each landmark, describing in a compact manner the type of structure in which it lies.¹⁷ Local feature vectors aim at characterizing the biological structure in which the point lies, whereas correlograms will put the points into context. Summarizing, associated to each

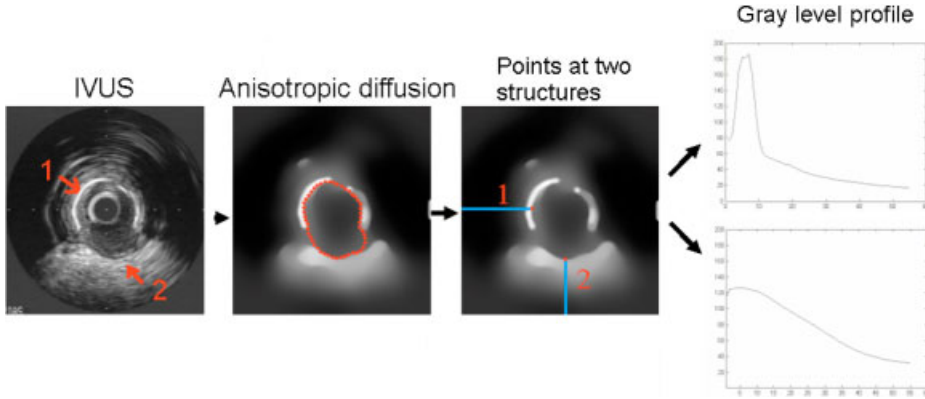


Figure 2. Landmark and local feature vector extraction.

characteristic point x_i we are going to use three different feature vectors: our local feature vector l_i , a 2-D correlogram v_i , and a 1-D correlogram w_i . We will now describe each of them in turn.

In IVUS images, regions such as calcium plaque are characterized by the gray level they have inside them and the gray level they cause outside them because of their echogenic impedance. Thus a good descriptor of the structure the point is at is the gray level profile along the line perpendicular to the wall from the point toward the outside part of the vessel (see Figure 2). We measure a set of statistics over this profile and its first derivative that conforms our local feature vector.¹

Correlograms are histograms that take into account relative spatial relations of the features. Centered at a particular point x_i , we measure the distribution of the local information regarding the rest of points along with their relative spatial distribution around x_i . Let C be a set of n landmarks. Let l_j be the label of the type of structure where the landmark x_j lies. Let n_c be the maximum number of classes. For x_i the correlogram v_i is defined as

$$v_i(r, \theta, c) = \#\{x_j \in C, x_j \neq x_i : \|x_j - x_i\| \in D_r, (\widehat{x_j - x_i}) \in A_\theta, l_j = c\} \quad (1)$$

where D_r is the r th interval of radius, $r = 1 \dots n_r$, A_θ is the θ th interval of angles, $\theta = 1 \dots n_\theta$, and c represents the class, $c = 1, \dots, n_c$. The sets of intervals $\{D_r\}_{r=1}^{n_r}$ and $\{A_\theta\}_{\theta=1}^{n_\theta}$ constitute a spatial quantization of the possible angles and possible distances of the relative positions around the current landmark. In Figure 3a we can see, superposed in white on an IVUS image, the spatial quantization associated to a bidimensional correlogram. This quantization of the spatial positions of the plane provides a partition in cells. The origin is taken as the landmark x_i . The red points are landmarks classified as belonging to plaque structure, whereas the blue points are landmarks classified as belonging to adventitia structure. The radial length of the cells grows at an exponential rate from the origin toward the outside, giving more importance to the near context of the point. This spatial quantization is the same as defined by Belongie et al.⁸

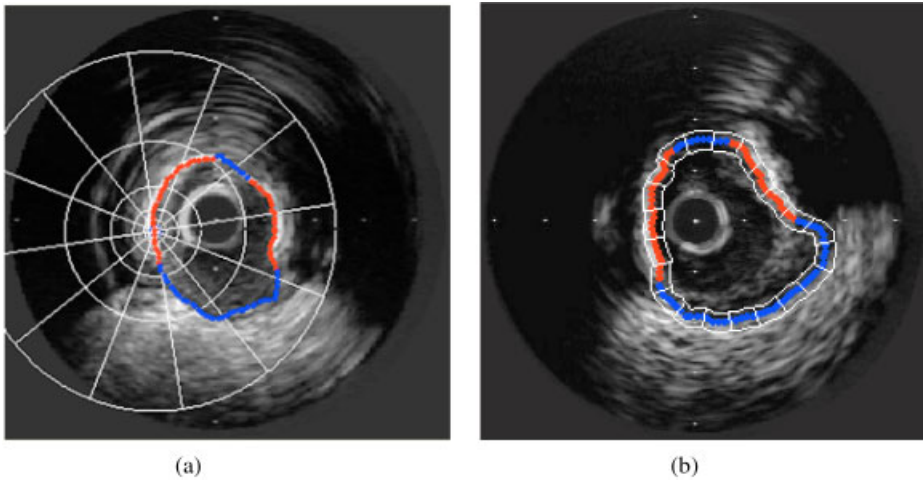


Figure 3. Bidimensional correlogram with 12 intervals of angles and 5 intervals of radius (a), and unidimensional correlogram (b).

The 1-D correlogram uses as spatial quantization a change of manifold from the whole plane to the contour curve where we have our characteristic points (see Figure 3b). We can express the contour curve as a function $\varphi: [0, 1) \rightarrow \mathbb{R}^2$ depending on an internal parameter $u \in [0, 1)$: $\varphi(u) = (x, y)$. We take as internal parameter u an approximation to the arc-length of the curve. Let $C_\Gamma = \{u_i\}_{i=1}^n$ be the set of arc-length parameters corresponding to the set of landmarks C . For x_i , its 1-D correlogram w_i is defined as

$$w_i(s, c) = \#\{u_j \in C_\Gamma, u_j \neq u_i : (u_j - u_i) \in I_s, l_j = c\} \quad (2)$$

where I_s is the interval of arc-length positions of the s th cell, $s = 1 \dots n_s$. By this definition, we are quantizing the possible values of arc-length differences between points of the curve. This difference must be computed with arithmetic modulus 1, in order to take into account the closed nature of the curve. The 1-D correlogram does not take into account the particular shape peculiarities of two structures to be aligned. In Figure 3b we can see, superposed in white on another IVUS image, the spatial quantization associated to a unidimensional correlogram. The red points are landmarks classified as belonging to plaque structure, whereas the blue points are landmarks classified as belonging to adventitia structure. In this picture, the cells have a constant length for clarity purposes. However, as in the bidimensional definition, the length of the cells grows at an exponential rate from the origin (the point x_i) toward the outside, giving more importance to the near context of the point.

We still can provide a different definition of our correlograms. Instead of measuring the spatial distribution of points belonging to different structures, we can measure the spatial distribution only of the points belonging to the same type

of structure as x_i . We call this other type of correlogram an autocorrelogram. This name is borrowed from Huang et al. for their color correlograms. For the 2-D spatial quantization, the 2-D autocorrelogram is

$$v_i(r, \theta, c) = \#\{x_j \in C, x_j \neq x_i : \|x_j - x_i\| \in D_r, (\widehat{x_j - x_i}) \in A_\theta, l_j = l_i\} \quad (3)$$

In the 1-D change of manifold, the 1-D autocorrelogram is

$$w_i(s) = \#\{u_j \in C_\Gamma, u_j \neq u_i : (u_j - u_i) \in I_s, l_j = l_i\} \quad (4)$$

Autocorrelograms are used for describing the spatial quantization of a particular type of structure without taking into account the rest of the structures. It allows us to describe global attributes such as the size of the structure without being disturbed by the distribution of the rest of the structures.

In this work we use 2-D correlograms (Equation 1) and 1-D autocorrelograms (Equation 4). In the registration algorithm, the 1-D autocorrelogram accounts mainly for the position of the point along the boundary of the structure it belongs to, saying intuitively if this point is at one extremum (and in which extremum it is) or if it is near the center of the structure. Thus extremum points from both structures are matched together, central points together, and so on. Once we have put the structures close by using the 2-D correlogram, which takes into account the 2-D distribution of structures, we finish an accurate matching of points from two analog structures by using the 1-D autocorrelogram.

The correlograms defined in this section are particular types of histograms. Many distances have been proven for these descriptors. We use in this work the χ^2 statistic. This is a distance normalized by the number of elements falling in the i bin of both histograms. It is not the same to have a difference of 5 elements if one bin has 1000 elements and the other 1005, as it is to have the same difference if one bin has 0 elements and the other 5. The latter difference is more significant. Thus for correlograms h_i and h_j we compute their distance as

$$\chi^2(h_i, h_j) = \frac{1}{2} \sum_{k=1}^d \frac{(h_i(k) - h_j(k))^2}{h_i(k) + h_j(k)}$$

where d is the number of bins of our correlograms. If we have a correlogram of dimension $n_r \times n_\theta \times n_c$ as in the 2-D case, we arrange the elements into a one-dimensional vector of $d \times 1$ elements where $d = n_r n_\theta n_c$. It is the same for the unidimensional definition of the correlogram.

3. REGISTRATION ALGORITHM: INVARIANCE TO ELASTIC TRANSFORMATIONS

The registration algorithm follows the point mapping paradigm¹⁸: Extract a set of characteristic points or landmarks from both images, then describe the landmarks in a feature space and compute the distance in the feature space between every pair of landmarks. Based on this distance we obtain a set of correspondences from landmarks in the first image (the *query image*) to landmarks in the second image (the *complementary image*) that globally minimizes the distance. The latter

is an assignment optimization algorithm, and can be resolved by the Hungarian's method.¹⁹ Finally, based on this set of correspondences we produce a transformation of the query image onto the complementary image. We make use of Thin-Plate Splines (TPS),^{20,21} which allows different degrees of approximation,²¹ making the transformation more coarse and global at initial steps and refining it locally in later steps. The degree of approximation/smoothing of the spline is controlled by a regularization parameter λ associated to this transformation.²¹

In the following we call the origin image I_1 and the destination image I_2 , so that the registration aligns I_1 to I_2 . First we apply a coarse alignment using as feature vectors only the 2-D correlograms, which accounts globally for the 2-D distribution of structures and puts analog structures close enough. The distance in this feature space is the χ^2 as explained in the previous section. Thus, the distance *in the feature space* between points $x_i \in I_1$ with 2-D correlogram v_i and $y_j \in I_2$ with 2-D correlogram v_j is $d_{ij}^f = \chi^2(v_i, v_j)$.

After this coarse alignment, we perform a more accurate alignment allowing more local and fine deformations. The second more accurate alignment is performed based on a combination of 1-D autocorrelograms and local feature vectors, and restricting the mapped points not to lie far away from mapped positions given by the coarse alignment. 1-D autocorrelograms are not as noisy as 2-D correlograms, but are only appropriate after a global alignment achieved by the use of the 2-D correlograms. In this fine alignment the distance *in the feature space* between $x_i \in I_1$ with 1-D autocorrelogram w_i and $y_j \in I_2$ with 1-D autocorrelogram w_j is computed as $d_{ij}^f = d_{class} + \chi^2(w_i, w_j)$, where d_{class} is infinite if both points do not belong to the same type of structure (class), and 0 if they do. By adding d_{class} we are restricting the correspondences to always match points belonging to the same structure.

Both transformations, the global and coarse first transformation and the more accurate second transformation, are obtained by a cooperative and iterative algorithm.¹⁸ This algorithm obtains a reliable set of correspondences based on correspondences that are not free of irregularities, and at the same time allows an accurate final alignment. The idea of cooperation between neighbor points is based on the fact that if one point x_i is matched with y_i , a neighbor point x_{i+1} of x_i should not be matched with a point y_j too far away from y_i . Let a couple of points $x_i \in I_1$ and $y_j \in I_2$, and let their distance in the feature space be d_{ij}^f . We have such a distance for every possible couple of points. After obtaining an initial set of correspondences based on the set of distances $\{d_{ij}^f\}$, we make a transformation by TPS. Let $f(x_i)$ be the mapping of x_i by the TPS. We recompute the distance between every pair of points ($x_i \in I_1, y_j \in I_2$) as

$$d_{ij} = d_{ij}^f + \alpha \|f(x_i) - y_j\| \quad (5)$$

We take $\{d_{ij}\}$ as the new set of distances and based on it we compute a new set of correspondences that produce a new transformation f . This new transformation f produces a new set of distances by Equation 5, and this is iterated several steps. The TPS do not allow two neighbor points x_{i+1} of x_i to be mapped far away from each other. Thus, by adding to the set of distances the term $\alpha \|f(x_i) - y_j\|$ for the

point x_i and $\alpha \|f(x_{i+1}) - y_j\|$ for the point x_{i+1} , we are biasing both points toward the same region of I_2 . The parameter α indicates how much we rely on the last transformation. If the last transformation is very accurate, we take as α a high value, restricting the corresponding points $y_j \in I_2$ to be near the mapped points $f(x_i)$. Thus, as the process makes the transformations better, we must increase this parameter through the successive iterations, beginning with a small value. The TPS transformation f has as a parameter a regularization degree λ . The higher the λ the more smooth the transformation, but the less approximation to the correspondences. A high λ is necessary in first steps when the correspondences are very irregular. The iterative algorithm makes the correspondences more and more regular, so that λ is decreased through the successive iterations. This at the same time makes the correspondences more and more accurate.

The explained iterative algorithm constitutes a feedback scheme similar to the one used by Chui and Rangarajan.²² However this algorithm is able to deal with gray-level images and does not need a deterministic annealing framework, as the combination of contextual and local descriptors gives us enough information to seek an accurate transformation in a more straightforward manner.

Finally, both types of correlograms depend on the spatial distribution of the characteristic points. As the spatial distribution of the points becomes modified by the successive mappings, we must recompute these correlograms through successive iterations of the algorithm.

4. COMPARISON BETWEEN PAIRS OF IMAGES: SIMILARITY MEASURE

The registration step gives us a transformation function T that maps every point x of I_1 to the domain $\Omega \subset \mathbb{R}^2$ of I_2 . From this transformation we must obtain a correspondence function $\phi: \{1, 2, \dots, n\} \rightarrow \{1, 2, \dots, m\}$, where $\{1, 2, \dots, n\}$ are the indexes of the characteristic points $\{x_1, x_2, \dots, x_n\}$ of I_1 , and $\{1, 2, \dots, m\}$ are the indexes of the characteristic points $\{y_1, y_2, \dots, y_m\}$ of I_2 . $\phi(i)$ must assign one index i to only one index j , but not necessarily all the indexes $i \in \{1, 2, \dots, n\}$ must be assigned because we allow outliers not to be matched to any point (see Ref. 17 for an explanation about how we deal with outliers). This function is computed by assigning to x_i the point from $\{y_1, y_2, \dots, y_m\}$ that lies more closely to its mapped position $T(x_i)$. This is achieved through the Hungarian's algorithm,¹⁹ the assignment method used before in the registration, but now taking as distance measures simply the Euclidean distance between mapped points $\{T(x_i)\}$ and destination points $\{y_j\}$.

Given the correspondence function ϕ computed, we compute the similarity between images I_1 and I_2 based on the feature vectors of the matched characteristic points. To be more precise, let $\{x_1, x_2, \dots, x_n\}$ be the set of characteristic points from I_1 and $\{y_1, y_2, \dots, y_m\}$ be the set of characteristic points from I_2 . Let f_{1i} be some feature vector (such as the local feature vector) associated to the i th characteristic point of the image I_1 , x_i . Let f_{2j} be the same kind of feature vector associated to the j th characteristic point of the image I_2 , y_j . The contribution of this type

f of feature vector to the distance between both images is $D_f = \sum_{i \in M_1} \|f_{1i} - f_{2\phi(i)}\|$, where $M_1 \subset \{1, 2, \dots, n\}$ is the subset of the indexes $\{1, 2, \dots, n\}$ associated to the characteristic points from I_1 that have any matching in ϕ , that is, indexes of points that are not considered outliers.

As explained before we have three types of feature vectors: local feature vectors, l , 2-D correlograms v , and 1-D autocorrelograms w . Local feature vectors account for the class of the region where the point lies, 2-D correlograms account for a distribution in the plane of the different regions around the current point, and 1-D autocorrelograms account for shape-invariant distributions of the regions along the boundary of the vessel, which allow us mainly to take into account characteristics such as the length of the calcium plaque regions where the points are located, as well as the position of the point along the region: in one extremum, in the middle, or in the center.

We let each of these types of feature vectors have its contribution distance to the total distance computed between the pair of images I_1 and I_2 . We also add into this distance the geometric distance between the mapped points of I_1 and their corresponding ones of I_2 , in order to know whether the two images have been allowed to match closely. This distance can be expressed as $D_{geom} = \sum_{i=1}^n \|T(x_i) - y_{\phi(i)}\|$. Finally we add a contribution from the energy of the deformation. High energy means a great degree of deformation for matching both images, indicating that the matching is not very natural. In summary, we have as distance between I_1 and I_2 a weighted sum of individual contributions: $D = \alpha_l D_l + \alpha_v D_v + \alpha_w D_w + \alpha_{geom} D_{geom} + \alpha_E D_E$, where D_l is the distance due to the local feature vector and α_l its weight, D_v is the distance due to the 2-D correlogram, α_v its weight, D_w is the distance due to the 1-D autocorrelogram, α_w its weight, and the other two distances and their α parameters take into account, respectively, the geometric distance and the energy of the deformation, and their weights. This set of weights is adjusted so that the retrieval result is optimal.

5. RESULTS

We show first the necessity of using contextual as well as local information and the necessity of using as contextual information not only the 2-D correlograms but also 1-D autocorrelograms. Then we provide quantitative results on retrieval of IVUS images using our approach.

Figure 4 shows a first couple of IVUS images with two calcium plaques, one on the left and the other one on the right. The IVUS image of Figure 4a corresponds to the query image, and the IVUS image of Figure 4b corresponds to its complementary image. In Figure 4c we show the anisotropic diffusion of the query image and superposed with dark contour the boundary of the vessel from which we extract the characteristic points. In Figure 4d we show the anisotropic diffusion of the complementary image and superposed in white the boundary of the vessel from which we extract the characteristic points.

In Figure 5 we compare the result of the first coarse transformation using contextual information (2-D correlograms) and using only local information (our local feature vectors). We show transformation results on the anisotropic diffusion

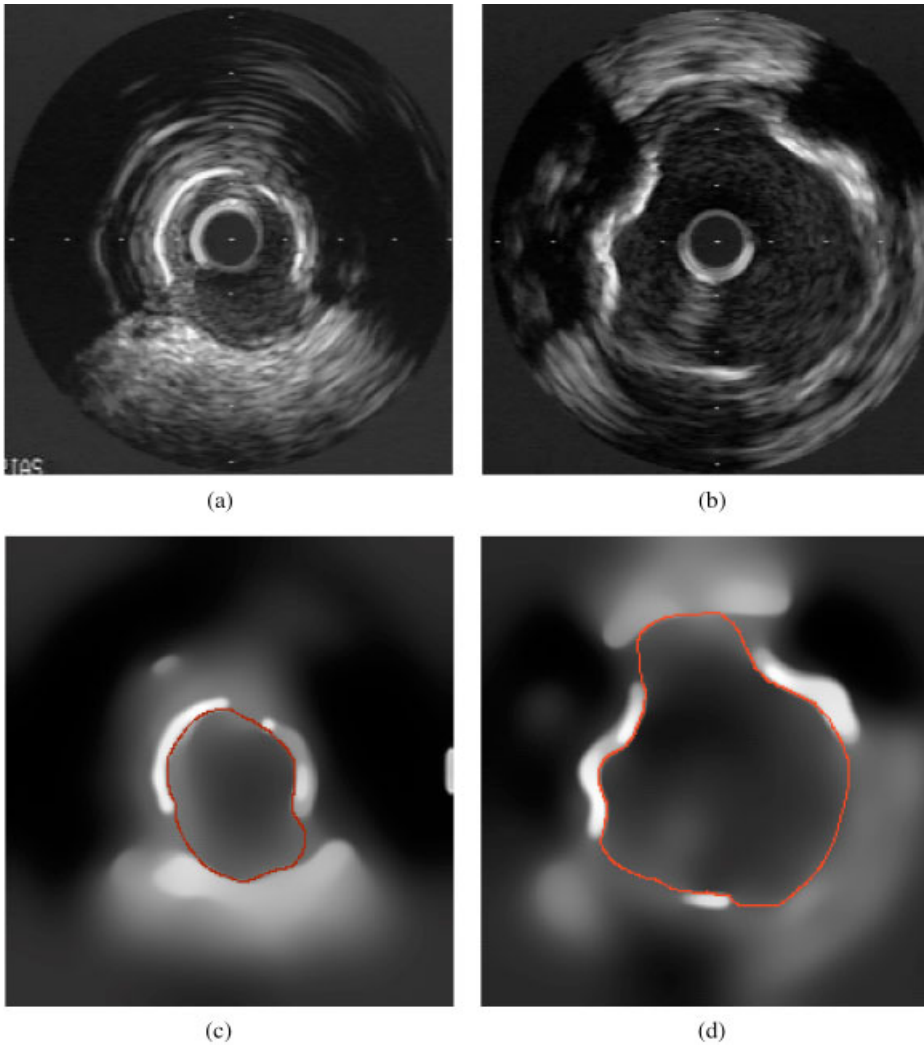


Figure 4. Query and its complementary IVUS (a, b). Their anisotropic diffusion results (c, d).

of the images because it is visually clearer. In Figure 5a we show the anisotropic diffusion of the query transformed by the coarse mapping. In Figure 5b we show the complementary image with the edges of the transformed query image superposed in white. We can see how both calcium plaques are mapped closely, as well as the adventitia tissue. In Figure 5c, d we show the same coarse transformation using only local feature vectors. We can see that one of the calcium plaques has not been mapped close to any of the calcium plaques of the complementary image.

Figure 6 shows how the set of correspondences using only a 2-D correlogram is more noisy than using a combination of 1-D autocorrelogram and local feature vectors.

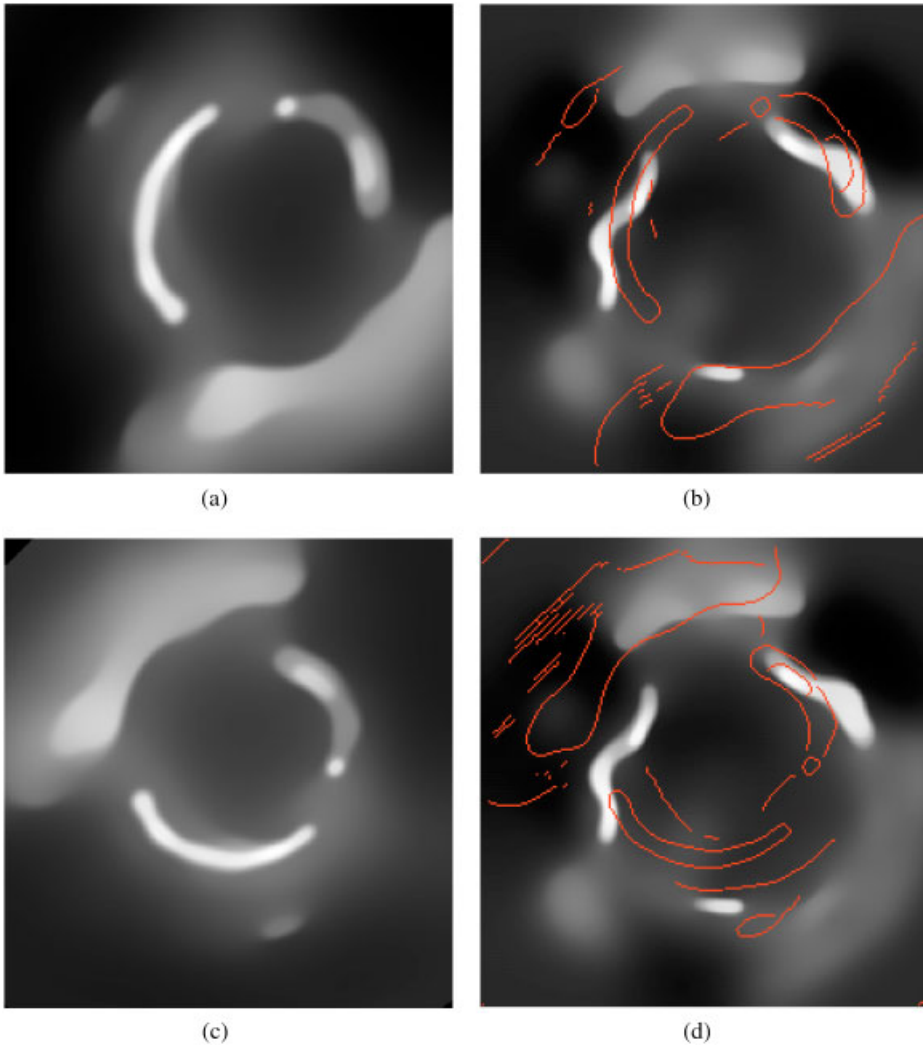


Figure 5. Coarse alignment (first step of the algorithm) using first contextual information (a,b), and then only local information (c,d).

In Figure 7 we compare the result of the transformation obtained in the second step using 1-D autocorrelograms and including the classification information by the distance d_{class} (see previous section), with a transformation obtained by the same algorithm but using 2-D correlograms and including also the classification information. As can be seen, the transformation using 2-D correlograms is more inaccurate and produces an irregular warping with the noise seen in the images. The irregular warping is due to be using a low regularization degree of the TPS based on too noisy a set of correspondences for such a small degree of regularization. In Figure 8 we see the final set of correspondences. Finally we see results for another couple in Figure 9.

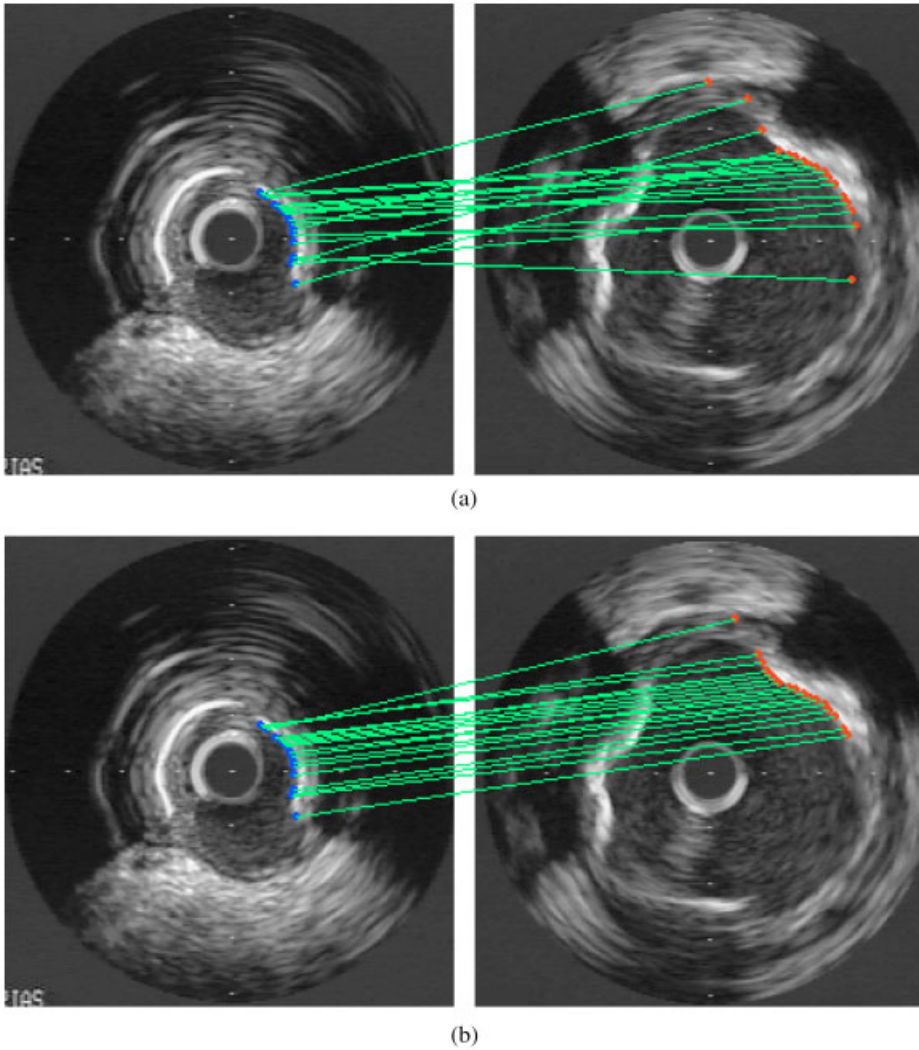


Figure 6. Correspondences with only 2-D correlograms (a) and correspondences with 1-D autocorrelograms and local feature vectors (b).

Now we give a series of quantitative results of our registration and retrieval system. Our database of IVUS images, collected for testing our system, comprise 168 images classified in two classes: images of diseased coronary vessels having calcium plaque and images of healthy vessels without any calcium plaque. Images with calcium plaque are further characterized by using a set of global descriptors whose values are assigned manually by physicians to each of the images, so that a complete dissimilarity measure between each pair of images can be computed based on a human's expert criteria. The characteristics used to discriminate among vessels with calcium are the length of the calcium plaque, the degree of embracement

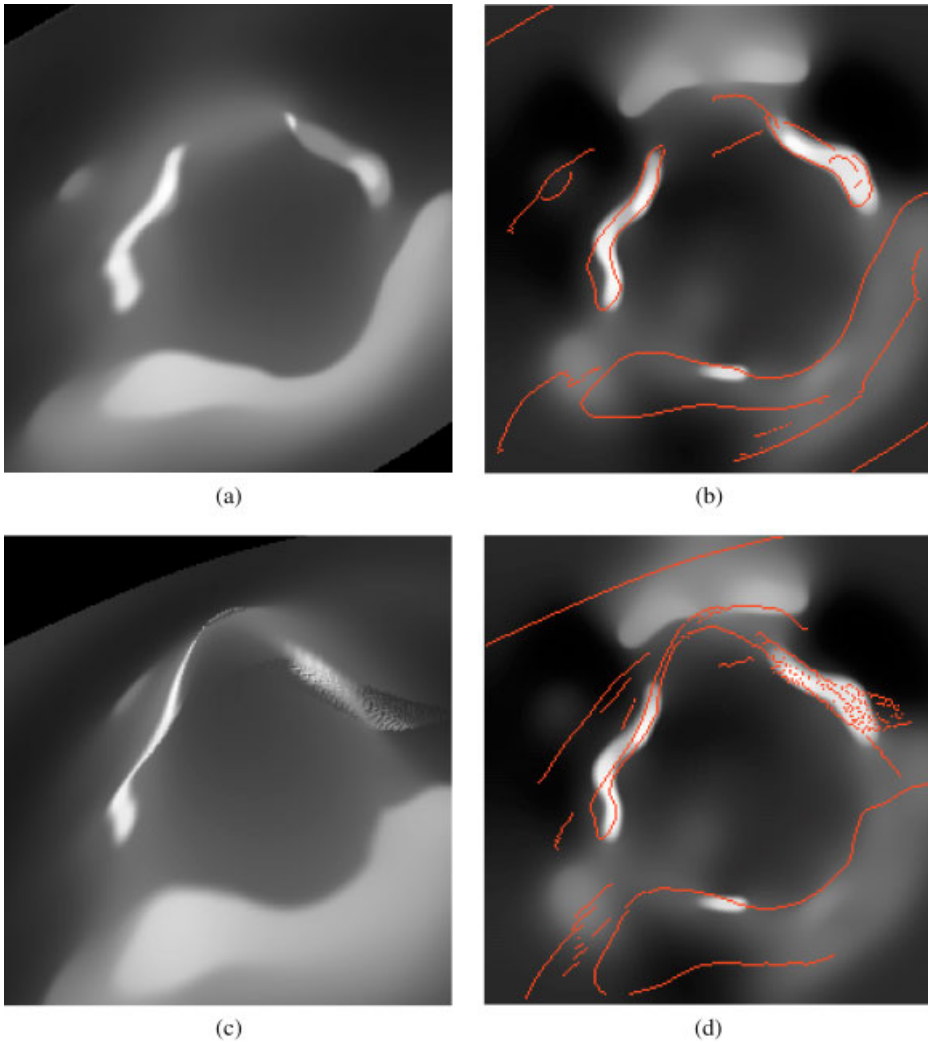


Figure 7. Second transformation using first 1-D autocorrelograms (a,b), and then 2-D correlograms (c, d).

of the plaque around the vessel, the number of plaques, and the thickness of the plaques. With this set of characteristics every image of a diseased vessel has a vector of characteristics assigned to it. We then compute the distance between every pair of images of diseased vessels as the euclidean of the vectors assigned to each of them. Although we are mainly interested in an accurate retrieval of images of diseased vessels, due to the clinical importance of determining the extent of the plaque, its disposition, and thickness, we also want our system to differentiate among diseased and healthy images. Thus half the set of images are from diseased vessels and the other half from healthy ones. We put the manual distance between any image from a diseased vessel and any image from a healthy image to a much

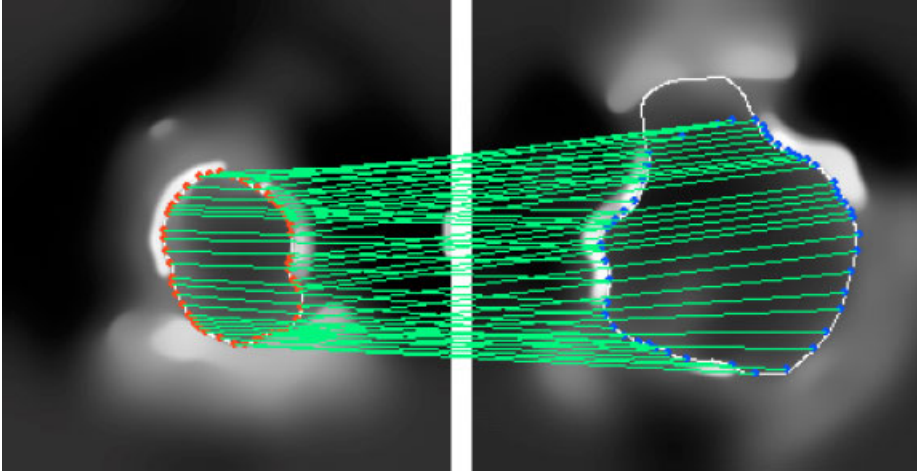


Figure 8. Final set of correspondences of the first pair of images.

higher value than any possible distance between two images of the same category. As we are not interested in discriminating between different IVUS images from healthy vessels we put the distance between every pair from the set of healthy vessel images to zero.

For assessing the rate of success of the retrieval system we use the physician-based dissimilarity measure explained above and see how close the automatic dissimilarity measure is to the assigned one. We present to the system a query image and use our retrieval similarity measure to assign a distance from every image from the database to the query. Then the images are sorted in increasing order of similarity, and the first most similar K images are presented to the user in order of similarity. We want to know what the value of K is for which an image very similar to the query is included. Let I_i be the query and I_j the complementary. We regard I_j as being very similar to the query if the physician-based dissimilarity measure $g(i, j)$ between both images is below a threshold. In our case this threshold is 1, as we have observed that below this threshold the similarity between the images is quite high. On average the value of K obtained through this procedure is 3. For $K = 2$ the percentage of times that one such image is included is 71%. In Figure 10 we can see three examples of retrieval. On the left we have the query image and on the right the three images most similar to the query. The weights obtained for the different distance components are $\alpha_l = 0.15$, $\alpha_v = 0.6$, $\alpha_w = 0.05$, $\alpha_E = 0.14$, and $\alpha_{geom} = 0.06$.

The frequency of times in which the first image selected is from the same category (diseased or healthy) as the query is 87.5%.

6. CONCLUSIONS AND FUTURE WORK

We apply registration and retrieval to a novel type of medical images, intravascular ultrasound (IVUS) images, images of highly elastic bodies that are quite

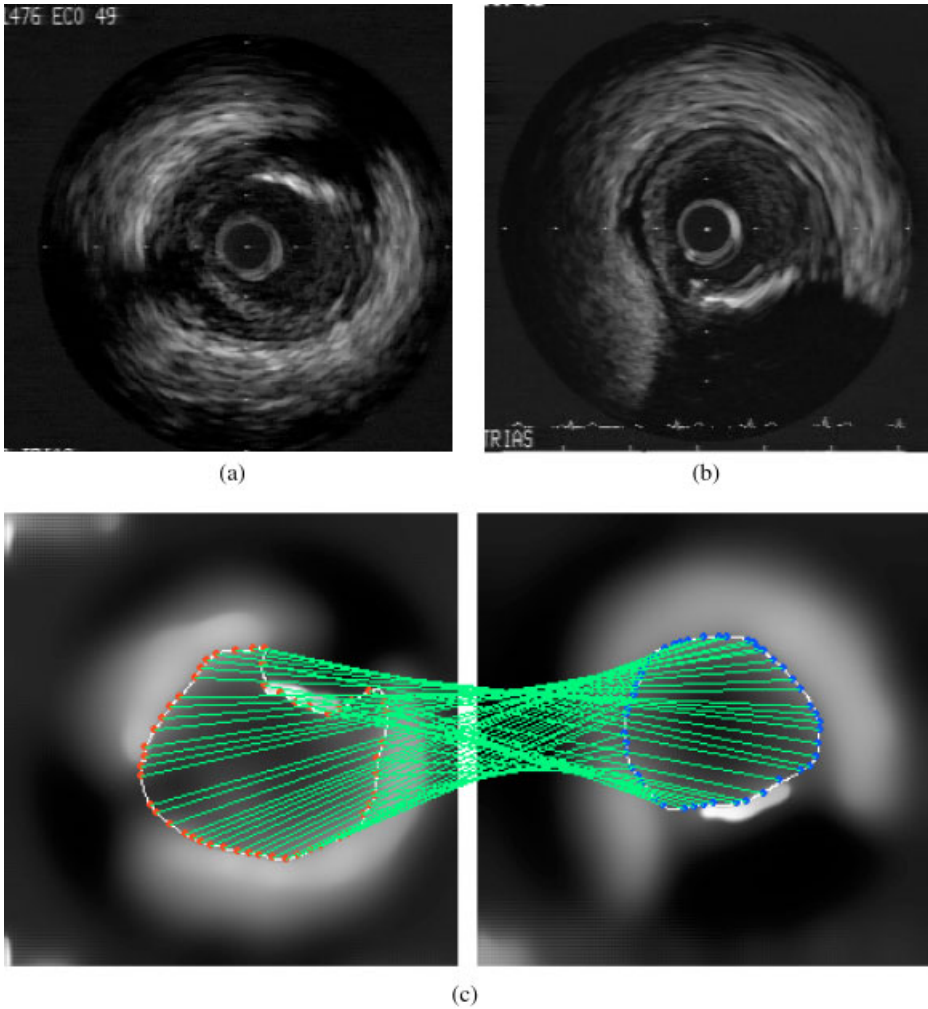


Figure 9. Query (a), complementary (b), and final set of correspondences on their anisotropic diffusions (c).

difficult to analyze. These types of images need a rich feature space, using not only local information around the point but also providing context or global information relative to this point. Instead of using graphs as a traditional technique, we extend the work of Belongie et al.⁸ using a modification of their correlograms in order to cope with gray-level images and adding a second contextual information, shape-invariant 1-D correlograms. In the registration algorithm we use this rich set of descriptors along with a cooperative-iterative scheme similar to the one used by Chui and Rangarajan,²² but designed to cope with gray-level images, and without the deterministic annealing framework they use, as the combination of contextual and local information gives us enough information to seek an accurate transformation in a more straightforward manner. The combination of rich

descriptors, a variational approach such as TPS, and the use of an iterative-cooperative scheme gives our registration algorithm robustness as well as accuracy, the result not depending on accurate classifications of all the points. The registration step provides invariance to elastic deformations of the object. It also provides measures of similarity for the registered images. We combine this registration with our generalized correlograms to obtain a robust and efficient retrieval comparison between images. Validated results are provided for a database of 168 IVUS images, showing the appropriateness of our method for images of such a high complexity.

As future work we must first include textural information in the computation of the local information, as we believe it fundamental in order to increase the richness of the descriptors and include more tissues. We want to work on a retrieval system in which first the set of possible images to match the query is filtered using rough descriptors. Then the registration would be done between a small set of images and the query, using a simple measure as the one explained above.

We are also investigating other variational approaches, apart from TPS, as TPS has the drawback that it does not differentiate between an irregular set of correspondences and a set of correspondences that lead to a high deformation of the object. We refer to Ref. 17 for a detailed explanation.

Acknowledgments

This work is supported by Ministerio de Ciencia y Tecnologia of Spain, grant TIC2000-1635-C04-04.

References

1. Pentland A, Picard RW, Sclaroff S. Photobook: Tools for content-based manipulation of image databases. In: Storage and retrieval for image and video databases. International Society for Optical Engineering; 1994. pp 34–47.
2. Flickner M, Sawhney H, Niblack W, Ashley J, Huang Q, Dom B, Gorkani M, Hafner J, Lee D, Petkovic D, Steele D, Yanker P. Query by image and video content: The qbic system. *IEEE Comput* 1995;28:23–32.
3. Carson C, Thomas M, Belongie S, Hellerstein JM, Malik J. Blobworld: A system for region-based image indexing and retrieval. In: Proc 3rd Int Conf on Visual Information Systems. Lecture Notes in Computer Science 1614. London: Springer-Verlag; 1999. pp 509–516.
4. Schmid C, Mohr R. Local grayvalue invariants for image retrieval. *IEEE Trans Pattern Anal Mach Intell* 1997;19:530–535.
5. Petrakis EGM, Faloutsos C. Similarity searching in medical image databases. *IEEE Trans Knowl Data Eng* 1997;9:435–447.
6. Chang SK, Yan CW, Dimitroff DC, Arndt T. An intelligent image database system. *IEEE Trans Software Engineering* 1988;14:681–688.
7. Huang J, Kumar S, Mitra M, Zhu W, Zabih R. Image indexing using color correlograms. In: Proc IEEE Conf Computer Vision and Pattern Recognition, San Juan, Puerto Rico, June 1997. pp 762–768.
8. Belongie S, Malik J, Puzicha J. Shape matching and object recognition using shape contexts. Technical Report UCB//CSD-00-1128. University of California, Berkeley, 2001.

9. Rao A, Srihari R, Zhang Z. Geometric histogram: A distribution of geometric configurations of color subsets. In: Beretta GB, Schettini R, editors. Proc SPIE: Internet Imaging 2000;3964:91–101.
10. Dahmen J, Theiner T, Keysers D, Ney H, Lehmann T, Wein B. Classification of radiographs in the image retrieval in medical applications system (IRMA). In: Proc 6th Int RIAO Conf on Content-Based Multimedia Information Access, Paris, 2000. pp 551–566.
11. Robinson GP, Tagare HD, Duncan JS, Jaffe CC. Medical image collection indexing: Shape-based retrieval using kd-trees. *Comput Med Imaging Graph* 1996;20:209–217.
12. Liu Y, Dellaert F, Rothfus WE, Moore A, Schneider J, Kanade T. Classification-driven pathological neuroimage retrieval using statistical asymmetry measures. In: Proc 2001 Medical Imaging Computing and Computer Assisted Intervention Conference (MICCAI '01), Utrecht, The Netherlands, October 2001. pp. 655–665.
13. Bajcsy R, Kovacic S. Multiresolution elastic matching. *Comput Vision Graph Image Process* 1989;46:1–21.
14. Boston Scientific Europe (ed.). Beyond angiography. Intravascular ultrasound: State of the art. vol. 1, XX Congress of the European Society of Cardiology, August 1998.
15. Weickert J. Anisotropic diffusion in image processing. Ph.D. thesis, Kaiserslautern University, 1996.
16. Bressan M, Vitria J. Nonparametric discriminant analysis and nearest neighbor classification. *Pattern Recogn Lett* 2003;24:2743–2749.
17. Amores J, Radeva, P. Elastic matching retrieval in medical images using contextual information. Technical report, Computer Vision Center, Barcelona, September 2003.
18. Brown L. A survey of image registration techniques. *ACM Comp Surv* 1992;24:325–376.
19. Papadimitriou C, Stieglitz K. Combinatorial optimization: Algorithms and complexity. Englewood Cliffs, NJ: Prentice Hall; 1982.
20. Bookstein FL. Principal warps: Thin-plate splines and the decomposition of deformations. *IEEE Trans Pattern Anal Mach Intell* 1989;11:567–585.
21. Wahba G. Spline models for observational data. Philadelphia, PA: Society for Industrial and Applied Math; 1990.
22. Chui H, Rangarajan A. A new algorithm for non-rigid point matching. In: Proc IEEE Conf Computer Vision and Pattern Recognition, Hilton Head, SC, June 13–15, 2000. pp 40–51.